

version, as from Xe_2Cl^* to XeCl^* , is also seen to ensure recombination (the minimum energy needed to again get free Kr^+ and Cl^- ions is 0.88 eV^{27}).

The behavior of the measured recombination rate constants and potential energy curves for both the $\text{Kr}_2^+/\text{Cl}^-/\text{Kr}$ and $\text{Xe}_2^+/\text{Cl}^-/\text{Xe}$ systems gives credence to our belief that the presented qualitative use of these curves can be used to determine if two-body electrostatic tidal recombination processes are important in gas-phase ionic recombination reactions. However, further attempts to predict this behavior in similar systems were inhibited by the lack of potential energy curves for the R_2X species in the literature.

At present, these calculations are being performed and along with the ionic recombination measurements will be reported in future publications.

Acknowledgment. We acknowledge the Australian Research Council for financial assistance during the course of this study.

References and Notes

- (1) Mezyk, S. P.; Cooper, R.; Sherwell, J. *J. Phys. Chem.* **1989**, *93*, 8187.
- (2) Mezyk, S. P.; Cooper, R.; Sherwell, J. *J. Phys. Chem.* **1991**, *95*, 3152.
- (3) Schmidt, W. F.; Jungblut, H.; Hansen, D.; Tagashira, H. *Proc. 6th Int. Conf. Gas. Dis. Applic., Heriot-Watt University* **1980**.
- (4) Sennhauser, E. S.; Armstrong, D. A. *J. Phys. Chem.* **1980**, *84*, 123.
- (5) See Bates, D. R. In *Advances in Atomic and Molecular Physics*; Bates, D. R., Bederson, B., Eds.; Academic Press: New York, 1985; Vol. 20, p 1, and references therein.

- (6) Langevin, P. *Ann. Chim. Phys.* **1903**, *28*, 433.
- (7) Harper, W. R. *Proc. Cambridge Philos. Soc.* **1932**, *28*, 219.
- (8) Bates, D. R.; Morgan, W. L. *Phys. Rev. Lett.* **1990**, *64*, 2258.
- (9) Young, J. Ph.D. Thesis, University of Melbourne, 1987.
- (10) Sherwell, J.; Cooper, R.; Nguyen, D. C.; Mezyk, S. P. *Aust. J. Chem.* **1988**, *41*, 1491 ($k = (1.54 \pm 0.09) \times 10^{14} \text{ M}^{-1} \text{ s}^{-1}$).
- (11) Smith, D.; Adams, N. G.; Alge, E. *J. Phys. B* **1984**, *17*, 461 ($k = (1.56 \pm 0.24) \times 10^{14} \text{ M}^{-1} \text{ s}^{-1}$).
- (12) Lacina, W. B.; Cohn, D. B. *Appl. Phys. Lett.* **1978**, *32*, 106.
- (13) Watanabe, K.; Nakayama, T.; Mottl, J. *J. Quant. Spectrosc. Radiat. Transfer* **1962**, *2*, 369.
- (14) Moore, C. E. *Analyses of Optical Spectra*; NSRDS-NBS 34; Office of Standard Reference Data, National Bureau of Standards: Washington, DC.
- (15) Murray, J. R.; Powell, H. T. *Appl. Phys. Lett.* **1976**, *29*, 252.
- (16) Grieser, F.; Shimamori, H. *J. Phys. Chem.* **1980**, *84*, 247.
- (17) Giles, K.; Adams, N. G.; Smith, D. *J. Phys. B* **1989**, *22*, 873.
- (18) Shuaibov, A. K.; Shevera, V. S. *Zh. Prikl. Spektrosk.* **1979**, *31*, 731.
- (19) Castex, M. C.; LeCalve, J.; Haaks, D.; Jordan, B.; Zimmerer, G. *Chem. Phys. Lett.* **1980**, *70*, 106.
- (20) Willis, C.; Boyd, A. W.; Young, M. J.; Armstrong, D. A. *Can. J. Chem.* **1970**, *48*, 1505.
- (21) Prosser, R. Ph.D. Thesis, University of Melbourne.
- (22) Ellis, H. W.; McDaniel, E. W.; Albrilton, D. L.; Viehland, L. A.; Lin, S. L.; Mason, E. A. *At. Data Nucl. Data Tables* **1978**, *22*, 179.
- (23) Bates, D. R.; Mendas, I. *Chem. Phys. Lett.* **1982**, *88*, 528.
- (24) Bates, D. R. *J. Phys. B* **1982**, *15*, L755.
- (25) Hay, P. J.; Dunning, T. H. Jr. *J. Chem. Phys.* **1978**, *69*, 2209.
- (26) Heustis, D. L. Presented at the 1979 Topical Meeting on Excimer Lasers, Charleston, SC, 1979.
- (27) Winter, N. W. "Comparison of KrCl and KrF Emission Spectra"; TAMP77-731, Lawrence Livermore National Laboratory, Livermore, CA, 1977.

Photoinduced Decarbonylation from Carbonyliron Tetraphenylporphyrin in Ethanol. Effects of Axial Imidazole Studied by Laser Flash Photolysis

Mikio Hoshino,*

The Institute of Physical and Chemical Research, Wako, Saitama 351-01, Japan

Koichi Ueda, Makoto Takahashi,

Faculty of Liberal Arts, International Christian University, Mitaka, Tokyo 181, Japan

Minoru Yamaji, Yoshimasa Hama,

Science and Engineering Laboratory, Waseda University, Shinjuku-ku, Tokyo 169, Japan

and Yoshio Miyazaki

Department of Chemistry, Toyo University, Kujirai, Kawagoe, Saitama 350, Japan (Received: April 2, 1992; In Final Form: July 24, 1992)

Photochemical reactions of carbonyliron(II) tetraphenylporphyrins, $(\text{CO})(\text{L})\text{Fe}^{\text{II}}\text{TPP}$ (L = ethanol and imidazole) and bisimidazoleiron(II) tetraphenylporphyrin, $(\text{Im})_2\text{Fe}^{\text{II}}\text{TPP}$, in ethanol were systematically investigated by laser flash photolysis. The yields for photodissociation of CO from $(\text{CO})(\text{C}_2\text{H}_5\text{OH})\text{Fe}^{\text{II}}\text{TPP}$ and $(\text{CO})(\text{Im})\text{Fe}^{\text{II}}\text{TPP}$ were determined to be 0.53 and 0.9 at room temperature, respectively. On the basis of the quantum yield measurements in the temperature range 180–300 K, the activation energies for decarbonylation obtained for $(\text{CO})(\text{C}_2\text{H}_5\text{OH})\text{Fe}^{\text{II}}\text{TPP}$ and $(\text{CO})(\text{Im})\text{Fe}^{\text{II}}\text{TPP}$ were 0 and 4.9 kcal mol^{-1} , respectively. No dissociation of the ligand L from $(\text{CO})(\text{L})\text{Fe}^{\text{II}}\text{TPP}$ was detected. The photochemical dissociation of the axial imidazole from $(\text{Im})_2\text{Fe}^{\text{II}}\text{TPP}$ was also studied. The yield for photodissociation of imidazole obtained was 0.18 at room temperature, and the activation energy was evaluated to be 2.6 kcal mol^{-1} . It was found that $(\text{Im})(\text{C}_2\text{H}_5\text{OH})\text{Fe}^{\text{II}}\text{TPP}$ produced by photolysis of both $(\text{CO})(\text{Im})\text{Fe}^{\text{II}}\text{TPP}$ and $(\text{Im})_2\text{Fe}^{\text{II}}\text{TPP}$ undergoes spontaneous base elimination to give $(\text{C}_2\text{H}_5\text{OH})_2\text{Fe}^{\text{II}}\text{TPP}$ and imidazole, Im. The reactive excited states responsible for photodissociation of the axial ligands as well as the spontaneous base elimination reaction are discussed in detail.

Introduction

In recent decades, the photochemistry of metalloporphyrins has been extensively investigated with the aid of the laser photolysis techniques which have proved of great use in the understanding of not only the excited state properties¹⁻⁵ but also of the dissociation and association mechanisms of axial ligands of the porphyrins.⁶⁻¹¹

In particular, the photochemistry of the O_2 , NO, and CO adducts of metalloporphyrins has aroused a great deal of attention as related to the elucidation of the nature of the binding between hemoproteins and simple diatomic molecules.¹²⁻²⁴

In 1979, White and his co-workers studied the photo-decarbonylation of carbonyliron(II) porphyrin which had nit-

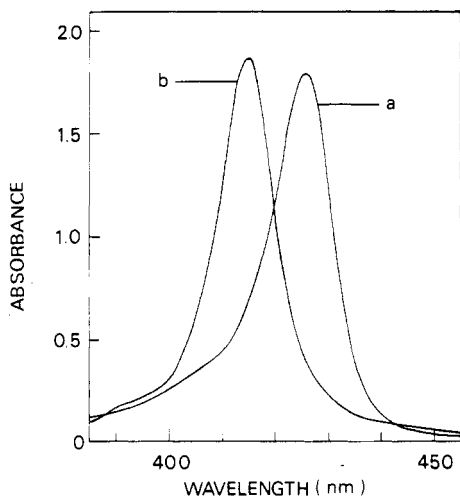


Figure 1. Absorption spectra of 5.35×10^{-6} M (a) $(\text{C}_2\text{H}_5\text{OH})_2\text{Fe}^{\text{II}}\text{TPP}$ and (b) $(\text{CO})(\text{C}_2\text{H}_5\text{OH})\text{Fe}^{\text{II}}\text{TPP}$ in ethanol.

rogenous bases for the sixth ligand in toluene.¹⁵ They found that the five-coordinate iron(II) porphyrin with an axial base produced after photoejection of CO undergoes spontaneous base elimination to give iron(II) porphyrin free from the axial base. Later, the base elimination pathway of the five-coordinate iron(II) porphyrin was confirmed by Lavalette and his co-workers.²⁵ However, owing to the complications of the reaction system, full understanding of all the rate constants for association and dissociation of ligands has not yet been achieved.

In the present paper, we report (1) the effects of temperature, excitation wavelengths, and axial ligands on the quantum yields for photodissociation of CO from $(\text{CO})(\text{L})\text{Fe}^{\text{II}}\text{TPP}$ in ethanol and (2) the spontaneous base elimination pathway that is discussed on the basis of the whole rate constants for the association and dissociation of the axial imidazole.

Experimental Section

Chloroiron(III) tetraphenylporphyrin, $\text{ClFe}^{\text{III}}\text{TPP}$, was synthesized according to the literature.²⁶ Reagent grade ethanol and imidazole, Im, supplied from Wako Pure Chem. Ind. Ltd. were used without further purification. Carbon monoxide (99.9%) from Takachiho Chem. Ind. Co. was used as supplied.

Sample solutions were degassed on a vacuum line by freeze-pump-thaw techniques to avoid oxygen contamination. Iron(II) tetraphenylporphyrin, $\text{Fe}^{\text{II}}\text{TPP}$, was prepared by photoreduction of $\text{ClFe}^{\text{III}}\text{TPP}$ in degassed ethanol.²⁷ The vacuum line was used for introduction of CO gas into the sample solutions.

Steady light photolysis was carried out with the use of a 250-W USH 250-D high-pressure mercury lamp. Absorption spectra were recorded on a Hitachi 330 spectrophotometer. Laser flash photolysis was performed with a Nd-YAG laser (Model HY 500 from JK Lasers Ltd.) equipped with second (532 nm), third (355 nm), and fourth (266 nm) harmonic generators. The detection system of the transient spectra was described elsewhere.²⁸ The temperatures of the sample solutions were controlled by a cryostat (Model DN704 from Oxford Instruments).

Quantum yields for photoreactions were determined by using the laser photolysis method which has been described in previous papers.^{6,7,13} The light intensity of the laser pulse was measured by monitoring the triplet-triplet absorption of zinc(II) tetraphenylporphyrin, $\text{Zn}^{\text{II}}\text{TPP}$, in a benzene solution: the molar absorption coefficient at 470 nm and the yield of the triplet $\text{Zn}^{\text{II}}\text{TPP}$ have been established as $7.3 \times 10^4 \text{ M}^{-1} \text{ cm}^{-1}$ and 0.83, respectively.²⁹ Laser pulses were defocused for determination of the quantum yields in order to minimize the saturation effects.

Results

Photodissociation of CO from Carbonyliron(II) Tetraphenylporphyrin in Ethanol. Figure 1 shows the absorption spectra of 5.33×10^{-6} M $(\text{C}_2\text{H}_5\text{OH})_2\text{Fe}^{\text{II}}\text{TPP}$ in ethanol before and after exposure to CO gas. The absorption peak of $(\text{C}_2\text{H}_5\text{OH})_2\text{Fe}^{\text{II}}\text{TPP}$

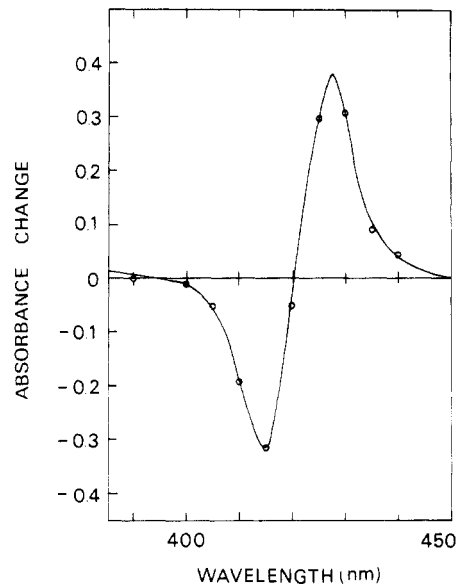
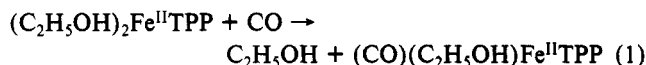


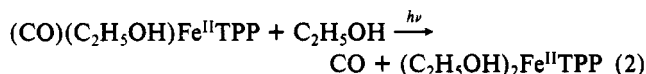
Figure 2. Transient absorption spectrum observed for an ethanol solution of $(\text{C}_2\text{H}_5\text{OH})\text{Fe}^{\text{II}}\text{TPP}$ detected at 50 ns after 355-nm laser pulsing. The pressure of CO gas is 200 Torr.

was instantaneously blue-shifted from 425 to 415 nm after introduction of CO into the solution:



The molar absorption coefficient of $(\text{CO})(\text{C}_2\text{H}_5\text{OH})\text{Fe}^{\text{II}}\text{TPP}$ was determined to be $3.5 \times 10^5 \text{ M}^{-1} \text{ cm}^{-1}$ at 415 nm.

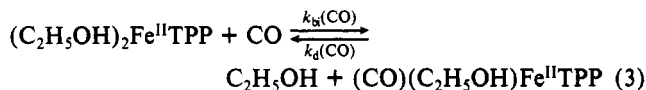
Figure 2 shows the transient absorption spectrum observed for the ethanol solution of $(\text{CO})(\text{C}_2\text{H}_5\text{OH})\text{Fe}^{\text{II}}\text{TPP}$ in a CO atmosphere ($P_{\text{CO}} = 200$ Torr), at 50 ns after 355 nm laser pulsing. The transient spectrum agrees well with the difference spectrum obtained by subtracting the spectrum of $(\text{CO})(\text{C}_2\text{H}_5\text{OH})\text{Fe}^{\text{II}}\text{TPP}$ from $(\text{C}_2\text{H}_5\text{OH})_2\text{Fe}^{\text{II}}\text{TPP}$, indicating that the following photo-reaction occurs:



The rate constant, k_{CO} , for regeneration of $(\text{CO})(\text{C}_2\text{H}_5\text{OH})\text{Fe}^{\text{II}}\text{TPP}$ is expressed as

$$k_{\text{CO}} = k_{\text{bi}}(\text{CO})[\text{CO}] + k_{\text{d}}(\text{CO}) \quad (i)$$

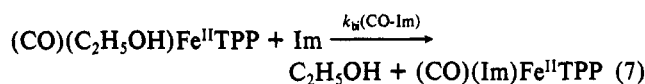
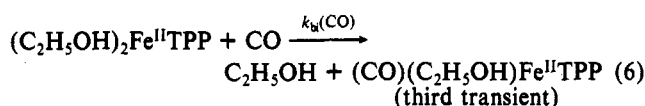
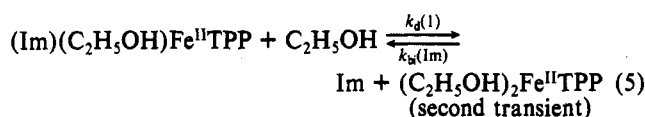
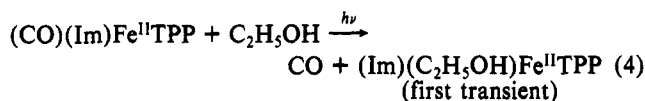
The transient decays according to first order kinetics with a rate constant $k_{\text{CO}} = 2.4 \times 10^4 \text{ s}^{-1}$. Because of the fact that $(\text{C}-\text{O})(\text{C}_2\text{H}_5\text{OH})\text{Fe}^{\text{II}}\text{TPP}$ is completely regenerated after photolysis, the decay process of the transient is described as



As shown in Figure 3, the plot of k_{CO} vs the CO pressure, P_{CO} , gives a straight line. From the slope of the line and the Ostwald solubility coefficient of CO in ethanol ($2.22 \times 10^{-2} \text{ atm}^{-1}$ at 303 K),³⁰ the bimolecular rate constant, $k_{\text{bi}}(\text{CO})$, between $(\text{C}_2\text{H}_5\text{O}-\text{H})_2\text{Fe}^{\text{II}}\text{TPP}$ and CO was determined as $1.0 \times 10^7 \text{ M}^{-1} \text{ s}^{-1}$ at 303 K. Since the intercept of the line is almost null, $k_{\text{d}}(\text{CO})$ is concluded to be negligible. Photodissociation of CO from $(\text{C}-\text{O})(\text{C}_2\text{H}_5\text{OH})\text{Fe}^{\text{II}}\text{TPP}$ was also observed with 532-nm laser photolysis.

Laser Photolysis of $(\text{CO})(\text{Im})\text{Fe}^{\text{II}}\text{TPP}$ at Low Imidazole Concentrations ($[\text{Im}] < 1.2 \times 10^{-2} \text{ M}$). With the addition of imidazole, the absorption spectrum of $(\text{CO})(\text{C}_2\text{H}_5\text{OH})\text{Fe}^{\text{II}}\text{TPP}$ in ethanol changes to that of $(\text{CO})(\text{Im})\text{Fe}^{\text{II}}\text{TPP}$: the molar absorption coefficient of $(\text{CO})(\text{Im})\text{Fe}^{\text{II}}\text{TPP}$ was obtained as $3.29 \times 10^5 \text{ M}^{-1} \text{ cm}^{-1}$ at the peak wavelength 420 nm.

Because of the complications of the photochemical reaction system, we initially studied the laser photolysis of (CO)(Im)-Fe^{II}TPP in ethanol at low imidazole concentrations. Figure 4 shows the transient spectra observed for an ethanol solution of 5.35×10^{-6} M (CO)(Im)Fe^{II}TPP in the presence of 7.3×10^{-4} M imidazole in a CO atmosphere ($P_{\text{CO}} = 200$ Torr), after 355-nm laser pulsing. Three transients were detected. The first transient spectrum observed at 50 ns after pulsing had the positive peak at 432 nm and the negative peak at 415 nm. It is transformed to the second one according to first order kinetics with a rate constant of 1.54×10^6 s⁻¹. The second transient spectrum further changes to the third one with a first order decay rate constant of 2.75×10^4 s⁻¹. The third transient goes back to (CO)(Im)-Fe^{II}TPP with the rate constant of 2×10^2 s⁻¹. From the transient spectra, the second and the third transient were, respectively, identified as (C₂H₅OH)₂Fe^{II}TPP and (CO)(C₂H₅OH)Fe^{II}TPP because (1) the second transient spectrum agrees well with the difference spectrum ((C₂H₅OH)₂Fe^{II}TPP - (CO)(Im)Fe^{II}TPP) and (2) the third transient spectrum with the positive and negative peaks at 415 and 420 nm, respectively, is in accord with the difference spectrum ((CO)(C₂H₅OH)Fe^{II}TPP - (CO)(Im)-Fe^{II}TPP). Since the first transient is a precursor of the second transient, (C₂H₅OH)₂Fe^{II}TPP, the first transient is probably ascribed to (Im)(C₂H₅OH)Fe^{II}TPP produced by the photolysis of (CO)(Im)Fe^{II}TPP. The spectral features, except for decay rates, of the transients detected at the imidazole concentrations, [Im], below 1.2×10^{-2} M were similar to those observed at [Im] = 7.3×10^{-4} M. Therefore, the photoreaction of (CO)(Im)-Fe^{II}TPP in ethanol, when [Im] < 1.2×10^{-2} M, can be described as follows.



We have measured the rate constant for the decay of each species by changing the pressure of CO and the concentration of imidazole, [Im]. On the assumption that $k_{\text{d}}(1) + k_{\text{bi}(\text{Im})}[\text{Im}] \gg k_{\text{bi}(\text{CO})}[\text{CO}] \gg k_{\text{bi}(\text{CO-Im})}[\text{Im}]$ at [Im] < 1.2×10^{-2} M, the decay rate constants k_{F} , k_{S} , and k_{T} , of the first, second, and third transients are, respectively, represented as

$$k_{\text{F}} = k_{\text{d}}(1) + k_{\text{bi}(\text{Im})}[\text{Im}] \quad (\text{ii})$$

$$k_{\text{S}} = k_{\text{bi}(\text{CO})}[\text{CO}] \quad (\text{iii})$$

$$k_{\text{T}} = k_{\text{bi}(\text{CO-Im})}[\text{Im}] \quad (\text{iv})$$

Figure 5 shows the plot of k_{F} vs [Im] in the concentration range $0 < [\text{Im}] < 1.2 \times 10^{-2}$ M. The rate constant k_{F} increases with an increase in [Im]:

$$k_{\text{F}} = 1.2 \times 10^6 + 1.1 \times 10^8 [\text{Im}] \text{ s}^{-1} \quad (\text{v})$$

From eq ii, we obtain $k_{\text{d}}(1) = 1.2 \times 10^6$ s⁻¹ and $k_{\text{bi}(\text{Im})} = 1.1 \times 10^8$ M⁻¹ s⁻¹. With the use of the values of $k_{\text{d}}(1)$ and $k_{\text{bi}(\text{Im})}$, the equilibrium constant K of the reaction 5 defined as $K_1 = k_{\text{bi}(\text{Im})}/k_{\text{d}}(1)$ is determined as 9.2×10 M⁻¹.

As exhibited in Figure 3, the decay rate constants, k_{S} , of the second transient represented as a function of the CO pressure are in good agreement with those obtained from the photolysis of

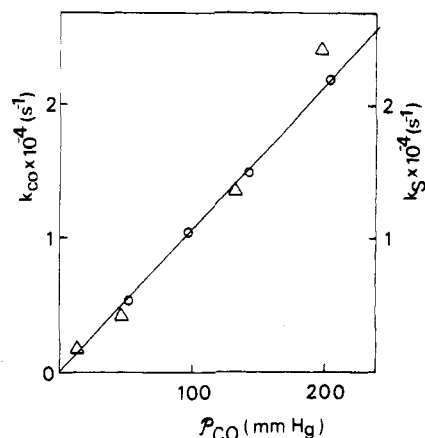


Figure 3. Decay rate constants, k_{CO} , of (C₂H₅OH)₂Fe^{II}TPP represented as a function of the pressure of CO gas. Open circles and triangles are the rate constants obtained with the laser photolysis of (CO)(C₂H₅OH)Fe^{II}TPP and (CO)(Im)Fe^{II}TPP, respectively (see text).

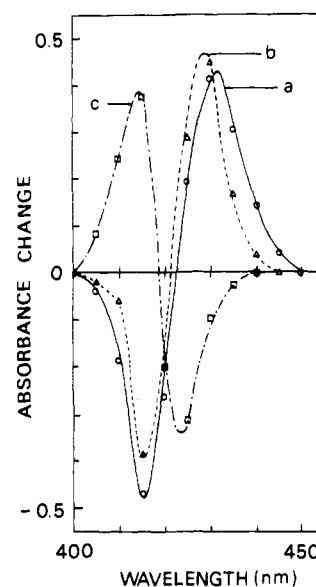


Figure 4. Transient absorption spectra observed for an ethanol solution of 5.35×10^{-6} M (CO)(Im)Fe^{II}TPP in the presence of 7.3×10^{-4} M imidazole, detected at (a) 50 ns, (b) 2.8 μs, and (c) 180 μs after 355-nm laser pulsing. The pressure of CO gas is 200 Torr.

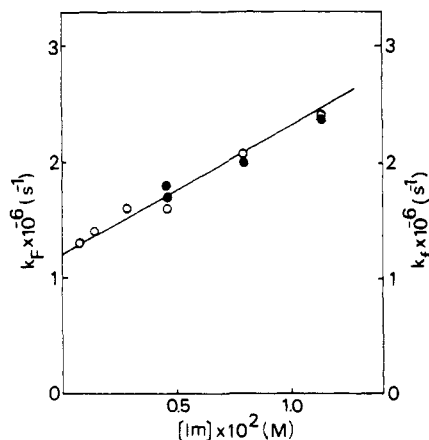


Figure 5. Decay rate constants of (Im)(C₂H₅OH)Fe^{II}TPP represented as a function of the imidazole concentration. Open and closed circles are, respectively, the rate constants k_{F} and k_{T} , determined by the laser photolysis studies of (CO)(Im)Fe^{II}TPP and (Im)₂Fe^{II}TPP in the presence of imidazole (see text). The CO gas pressure is 200 Torr.

(CO)(C₂H₅OH)Fe^{II}TPP: $k_{\text{bi}(\text{CO})} = 1.0 \times 10^7$ M⁻¹ s⁻¹. This result supports the conclusion that the second transient is (C₂H₅OH)₂Fe^{II}TPP. It was found that the rate constants for the

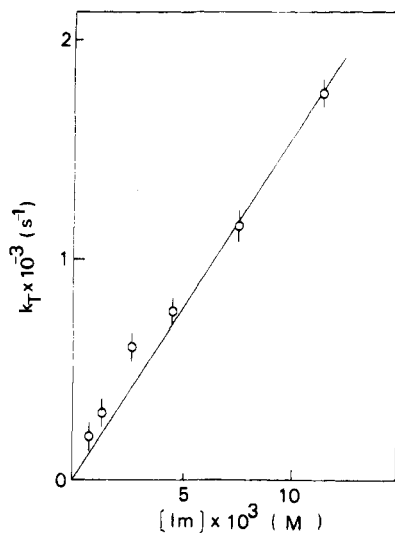


Figure 6. Decay rate constant, k_T , of $(\text{CO})(\text{C}_2\text{H}_5\text{OH})\text{Fe}^{\text{II}}\text{TPP}$ represented as a function of the imidazole concentration. The CO gas pressure is 200 Torr.

decay of the first and third transient spectra are almost independent of the CO pressure.

Figure 6 shows the rate constant, k_T , for the decay of the third transient represented as a function of imidazole, $[\text{Im}]$, in the concentration range $0 < [\text{Im}] < 1.2 \times 10^{-2}$ M. The plot of k_T vs $[\text{Im}]$ gives a straight line:

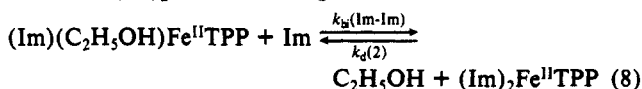
$$k_T = 1.52 \times 10^5 [\text{Im}] \text{ s}^{-1} \quad (\text{vi})$$

From eq iv, the bimolecular rate constant, $k_{\text{bi}}(\text{Im})$, obtained was $1.52 \times 10^5 \text{ M}^{-1} \text{ s}^{-1}$.

For the derivation of eqs ii-iv, the assumptions mentioned above were used. These assumption are justified under the present experimental conditions, $P_{\text{CO}} = 200$ Torr and $[\text{Im}] < 1.2 \times 10^{-2}$ M, because $k_d(1) + k_{\text{bi}}(\text{Im})[\text{Im}] > k_d(1) = 1.2 \times 10^6 \text{ s}^{-1} \gg k_{\text{bi}}(\text{CO})[\text{CO}] = 2.75 \times 10^4 \text{ s}^{-1} \gg k_{\text{bi}}(\text{CO-Im})[\text{Im}] = 1.8 \times 10^3 \text{ s}^{-1}$.

In the reactions 5-7 described above, the equilibrium reaction between $(\text{Im})(\text{C}_2\text{H}_5\text{OH})\text{Fe}^{\text{II}}\text{TPP}$ and $(\text{Im})_2\text{Fe}^{\text{II}}\text{TPP}$ was ignored because of the fact that no formation of $(\text{Im})_2\text{Fe}^{\text{II}}\text{TPP}$ was observed at low imidazole concentrations.

Laser Photolysis of $(\text{CO})(\text{Im})\text{Fe}^{\text{II}}\text{TPP}$ at High Imidazole Concentrations ($[\text{Im}] > 2 \times 10^{-2}$ M). Figure 7 shows the transient absorption spectra observed for an ethanol solution of 5.35×10^{-6} M $(\text{CO})(\text{Im})\text{Fe}^{\text{II}}\text{TPP}$ in the presence of 8.15×10^{-2} M imidazole in a CO atmosphere ($P_{\text{CO}} = 200$ Torr), by 355-nm laser photolysis. Two transients were observed. The first transient spectrum initially detected 50 ns after pulsing is identical with the spectrum shown in Figure 4, indicating that the transient is $(\text{Im})(\text{C}_2\text{H}_5\text{OH})\text{Fe}^{\text{II}}\text{TPP}$. The first transient changes to the second one according to first order kinetics with a rate constant of $5.0 \times 10^5 \text{ s}^{-1}$. It is found that the second transient spectrum agrees well with the difference spectrum obtained by subtracting the spectrum of $(\text{CO})(\text{Im})\text{Fe}^{\text{II}}\text{TPP}$ from that of $(\text{Im})_2\text{Fe}^{\text{II}}\text{TPP}$ which, as will be mentioned later, is prepared by the addition of 6.6×10^{-2} M imidazole into the ethanol solution of 5.35×10^{-6} M $(\text{C}_2\text{H}_5\text{O-H})_2\text{Fe}^{\text{II}}\text{TPP}$. This finding implies that the first transient, $(\text{Im})(\text{C}_2\text{H}_5\text{OH})\text{Fe}^{\text{II}}\text{TPP}$, reacts with imidazole to yield the second transient, $(\text{Im})_2\text{Fe}^{\text{II}}\text{TPP}$, at high concentrations of imidazole:



The plot of the decay rate constant of $(\text{Im})(\text{C}_2\text{H}_5\text{OH})\text{Fe}^{\text{II}}\text{TPP}$ vs $[\text{Im}]$ gave a straight line in the concentration region $[\text{Im}] > 2 \times 10^{-2}$ M. From the slope of the line, we obtained $k_{\text{bi}}(\text{Im-Im}) = 6.25 \times 10^6 \text{ M}^{-1} \text{ s}^{-1}$. The intercept of the line is close to zero, suggesting that $k_d(2)$ and the rate for the reaction between $(\text{Im})(\text{C}_2\text{H}_5\text{OH})\text{Fe}^{\text{II}}\text{TPP}$ and CO are negligibly small in comparison with $k_{\text{bi}}(\text{Im-Im})[\text{Im}]$.

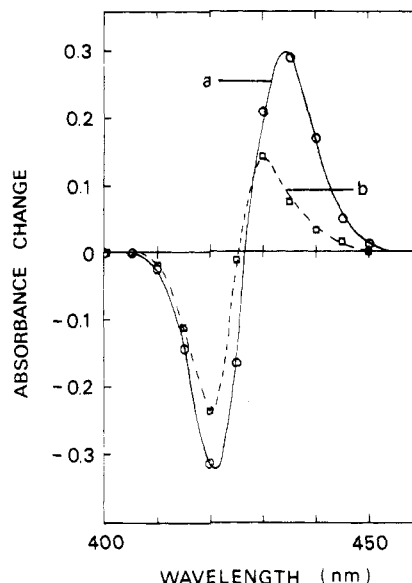
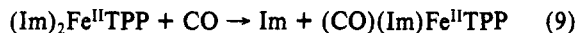


Figure 7. Transient absorption spectra observed for an ethanol solution of 5.35×10^{-6} M $(\text{CO})(\text{Im})\text{Fe}^{\text{II}}\text{TPP}$ in the presence of 8.15×10^{-2} M imidazole, detected at (a) 50 ns and (b) 7.5 μs after 355-nm laser pulsing. The CO gas pressure is 200 Torr.

The second transient, $(\text{Im})_2\text{Fe}^{\text{II}}\text{TPP}$, decays with the pseudo first order rate constant of $2.5 \times 10^2 \text{ s}^{-1}$ owing to the recombination reaction with CO to regenerate $(\text{CO})(\text{Im})\text{Fe}^{\text{II}}\text{TPP}$:



The decay rate of $(\text{Im})_2\text{Fe}^{\text{II}}\text{TPP}$ increased with increasing CO pressure while it decreased with increasing concentration of imidazole. This fact suggests that, although $(\text{Im})_2\text{Fe}^{\text{II}}\text{TPP}$ itself is not reactive toward CO, the reaction observed in this case between CO and $(\text{Im})_2\text{Fe}^{\text{II}}\text{TPP}$ can be made via $(\text{Im})(\text{C}_2\text{H}_5\text{OH})\text{Fe}^{\text{II}}\text{TPP}$ and/or $(\text{C}_2\text{H}_5\text{OH})_2\text{Fe}^{\text{II}}\text{TPP}$ which are expected to be in equilibrium with $(\text{Im})_2\text{Fe}^{\text{II}}\text{TPP}$ in ethanol.

The transient species $(\text{C}_2\text{H}_5\text{OH})_2\text{Fe}^{\text{II}}\text{TPP}$ could not be detected by laser photolysis of $(\text{Im})_2\text{Fe}^{\text{II}}\text{TPP}$ at $[\text{Im}] = 8.15 \times 10^{-2}$ M. This fact is interpreted as follows. (1) The rate constant for achievement of the equilibrium 5, $k_d(1) + k_{\text{bi}}(\text{Im})[\text{Im}]$, is as large as 10^7 s^{-1} at $[\text{Im}] = 8.15 \times 10^{-2}$ M. (2) From the equilibrium constant, $K_1 = k_{\text{bi}}(\text{Im})/k_d(1) = 9.2 \times 10^{-1}$ M, for the equilibrium 5, the ratio, $[(\text{Im})(\text{C}_2\text{H}_5\text{OH})\text{Fe}^{\text{II}}\text{TPP}]/[(\text{C}_2\text{H}_5\text{OH})_2\text{Fe}^{\text{II}}\text{TPP}]$, at $[\text{Im}] = 8.15 \times 10^{-2}$ M is calculated as 7.5. Thus, the major species after rapid establishment of the equilibrium 5 is $(\text{Im})(\text{C}_2\text{H}_5\text{OH})\text{Fe}^{\text{II}}\text{TPP}$.

Quantum Yield Measurements for Photodissociation of CO. Laser photolysis of $(\text{CO})(\text{C}_2\text{H}_5\text{OH})\text{Fe}^{\text{II}}\text{TPP}$ in ethanol liberates CO to yield $(\text{C}_2\text{H}_5\text{OH})_2\text{Fe}^{\text{II}}\text{TPP}$. Since the molar absorption coefficients of authentic $(\text{C}_2\text{H}_5\text{OH})_2\text{Fe}^{\text{II}}\text{TPP}$ can be measured, the quantum yield for photodissociation of CO from $(\text{CO})(\text{C}_2\text{H}_5\text{OH})\text{Fe}^{\text{II}}\text{TPP}$ was readily obtained to be 0.54 ± 0.05 at both 355 and 532 nm with the laser photolysis method.

The laser photolysis studies revealed that $(\text{CO})(\text{Im})\text{Fe}^{\text{II}}\text{TPP}$ at $[\text{Im}] = 7.3 \times 10^{-4}$ and at $P_{\text{CO}} = 200$ Torr also photodissociates CO to give three transient species, $(\text{Im})(\text{C}_2\text{H}_5\text{OH})\text{Fe}^{\text{II}}\text{TPP}$, $(\text{C}_2\text{H}_5\text{OH})_2\text{Fe}^{\text{II}}\text{TPP}$, and $(\text{CO})(\text{Im})\text{Fe}^{\text{II}}\text{TPP}$. The molar absorption coefficient of authentic $(\text{Im})(\text{C}_2\text{H}_5\text{OH})\text{Fe}^{\text{II}}\text{TPP}$, as will be shown later, could not be obtained, and, therefore, direct determination of the dissociation yield of CO from $(\text{CO})(\text{Im})\text{Fe}^{\text{II}}\text{TPP}$ was unsuccessful. However, we have the absorption spectra of authentic $(\text{C}_2\text{H}_5\text{OH})_2\text{Fe}^{\text{II}}\text{TPP}$ and $(\text{CO})(\text{C}_2\text{H}_5\text{OH})\text{Fe}^{\text{II}}\text{TPP}$. The yields for the formation of $(\text{C}_2\text{H}_5\text{OH})_2\text{Fe}^{\text{II}}\text{TPP}$ and $(\text{CO})(\text{C}_2\text{H}_5\text{OH})\text{Fe}^{\text{II}}\text{TPP}$ were, respectively, determined to be 0.9 ± 0.1 and 0.8 ± 0.1 . Because $(\text{Im})(\text{C}_2\text{H}_5\text{OH})\text{Fe}^{\text{II}}\text{TPP}$ is a precursor of $(\text{C}_2\text{H}_5\text{OH})_2\text{Fe}^{\text{II}}\text{TPP}$, the yield for photodissociation of CO from $(\text{CO})(\text{Im})\text{Fe}^{\text{II}}\text{TPP}$ is estimated as 0.9 ± 0.1 on the assumption that $(\text{Im})(\text{C}_2\text{H}_5\text{OH})\text{Fe}^{\text{II}}\text{TPP}$ dissociates Im with the yield of unity.

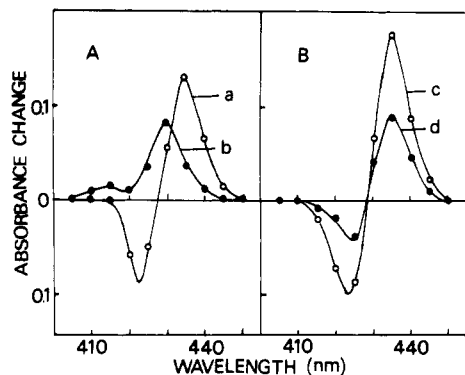
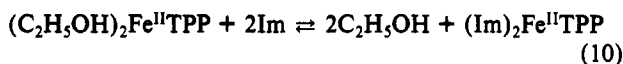


Figure 8. Transient absorption spectra observed for ethanol solutions of 5.35×10^{-6} M $(\text{Im})_2\text{Fe}^{\text{II}}\text{TPP}$ in the presence of (A) 4.57×10^{-3} M and (B) 4.57×10^{-2} M imidazole, detected at (a) 50 ns, (b) 2 μ s, (c) 50 ns, and (d) 1 μ s after 355-nm laser pulsing.

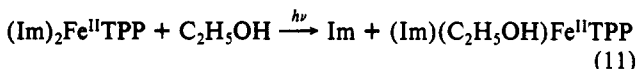
Photodissociation of Axial Imidazole from $(\text{Im})_2\text{Fe}^{\text{II}}\text{TPP}$. For further elucidation of the decay behavior of $(\text{C}_2\text{H}_5\text{OH})_2\text{Fe}^{\text{II}}\text{TPP}$, $(\text{Im})(\text{C}_2\text{H}_5\text{OH})\text{Fe}^{\text{II}}\text{TPP}$, and $(\text{Im})_2\text{Fe}^{\text{II}}\text{TPP}$ detected by laser photolysis of $(\text{CO})(\text{Im})\text{Fe}^{\text{II}}\text{TPP}$, we have studied the photochemistry of $(\text{Im})_2\text{Fe}^{\text{II}}\text{TPP}$ in ethanol.

The absorption spectral changes of $(\text{C}_2\text{H}_5\text{OH})_2\text{Fe}^{\text{II}}\text{TPP}$ in ethanol by the addition of imidazole exhibited isosbestic points in both the Q and the Soret band region in the concentration range studied $0 < [\text{Im}] < 8.15 \times 10^{-2}$ M. It, therefore, is suggested that $(\text{C}_2\text{H}_5\text{OH})_2\text{Fe}^{\text{II}}\text{TPP}$ is in equilibrium with a single species. The spectral change was interpreted in terms of the following equilibrium reaction:



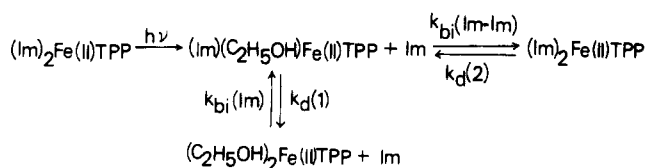
The equilibrium constant K obtained from the spectral changes is $K = 2.0 \times 10^5 \text{ M}^{-2}$. Because of the formation of $(\text{Im})_2\text{Fe}^{\text{II}}\text{TPP}$, the absorption peak of $(\text{C}_2\text{H}_5\text{OH})_2\text{Fe}^{\text{II}}\text{TPP}$ located at 425 nm in the Soret band region merely decreased with an increase in the concentration of imidazole. The molar absorption coefficient of $(\text{Im})_2\text{Fe}^{\text{II}}\text{TPP}$ was determined as $2.52 \times 10^5 \text{ M}^{-1} \text{ cm}^{-1}$ at 425 nm. We could not spectroscopically detect the formation of $(\text{Im})(\text{C}_2\text{H}_5\text{OH})\text{Fe}^{\text{II}}\text{TPP}$ in the concentration range $[\text{Im}] < 1 \times 10^{-2}$ M. Presumably, the steady state concentration of $(\text{Im})(\text{C}_2\text{H}_5\text{OH})\text{Fe}^{\text{II}}\text{TPP}$, which is considered to be an intermediate in the equilibrium reaction described above, is very low owing to its instability in ethanol. Brault and Rougee have studied ligand binding between iron(II) porphyrin and pyridine in ethanol.³¹ They found that iron(II) porphyrin binds two pyridine molecules with the equilibrium constant $K = 1.6 \times 10^5 \text{ M}^{-2}$ with its value being close to that obtained with the equilibrium reaction 10.

Figure 8 shows the transient absorption spectra observed for ethanol solutions of $(\text{C}_2\text{H}_5\text{OH})_2\text{Fe}^{\text{II}}\text{TPP}$ containing (a) 4.57×10^{-3} and (b) 4.7×10^{-2} M imidazole, after 355-nm laser pulsing. The first transient detected at 50 ns for both solutions is ascribed to $(\text{Im})(\text{C}_2\text{H}_5\text{OH})\text{Fe}^{\text{II}}\text{TPP}$ produced by photodissociation of an axial imidazole:



For the ethanol solution containing 4.57×10^{-3} M imidazole, the first transient, $(\text{Im})(\text{C}_2\text{H}_5\text{OH})\text{Fe}^{\text{II}}\text{TPP}$, changes to the second one, $(\text{C}_2\text{H}_5\text{OH})_2\text{Fe}^{\text{II}}\text{TPP}$, with a first order rate constant, $k_f = 1.7 \times 10^6 \text{ s}^{-1}$. The second transient further decays with the first order rate constant, $k_s = 1.72 \times 10^6 \text{ s}^{-1}$, to regenerate $(\text{Im})_2\text{Fe}^{\text{II}}\text{TPP}$. With the increase in the concentration of imidazole, k_f increased and the spectral changes from the first to the second transient became undiscernible. In fact, $(\text{Im})(\text{C}_2\text{H}_5\text{OH})\text{Fe}^{\text{II}}\text{TPP}$ observed in an ethanol solution containing 4.7×10^{-2} M imidazole only disappears with the first order rate constant $k_s = 3.2 \times 10^5 \text{ s}^{-1}$ to regenerate $(\text{Im})_2\text{Fe}^{\text{II}}\text{TPP}$. The photoreaction of $(\text{Im})_2\text{Fe}^{\text{II}}\text{TPP}$ and the subsequent reactions are described in Scheme I. The time-dependent spectral changes of $(\text{Im})(\text{C}_2\text{H}_5\text{OH})\text{Fe}^{\text{II}}\text{TPP}$ ob-

SCHEME I



served here are interpreted in terms of the equilibrium reactions shown in Scheme I: (1) at low imidazole concentrations, $(\text{Im})(\text{C}_2\text{H}_5\text{OH})\text{Fe}^{\text{II}}\text{TPP}$ dissociates Im with the rate constant, k_f , to yield $(\text{C}_2\text{H}_5\text{OH})_2\text{Fe}^{\text{II}}\text{TPP}$ as major species according to the first equilibrium between $(\text{Im})(\text{C}_2\text{H}_5\text{OH})\text{Fe}^{\text{II}}\text{TPP}$ and $(\text{C}_2\text{H}_5\text{OH})_2\text{Fe}^{\text{II}}\text{TPP}$ and, after that, the first equilibrium shifts to the second equilibrium between $(\text{Im})(\text{C}_2\text{H}_5\text{OH})\text{Fe}^{\text{II}}\text{TPP}$ and $(\text{Im})_2\text{Fe}^{\text{II}}\text{TPP}$ with the rate constant, k_s , while at high imidazole concentrations, the dissociation of Im from $(\text{Im})(\text{C}_2\text{H}_5\text{OH})\text{Fe}^{\text{II}}\text{TPP}$ is suppressed and, therefore, time-dependent spectral changes from $(\text{Im})(\text{C}_2\text{H}_5\text{OH})\text{Fe}^{\text{II}}\text{TPP}$ to $(\text{C}_2\text{H}_5\text{OH})_2\text{Fe}^{\text{II}}\text{TPP}$ after pulsing become undetectable. It is confirmed that $(\text{Im})(\text{C}_2\text{H}_5\text{OH})\text{Fe}^{\text{II}}\text{TPP}$ produced by photolysis of $(\text{Im})_2\text{Fe}^{\text{II}}\text{TPP}$ achieves the second equilibrium after establishment of the first equilibrium: $k_d(1) + k_{bi}(\text{Im})[\text{Im}] \gg k_d(2) + k_{bi}(\text{Im}-\text{Im})[\text{Im}]$.

From the above considerations, the initial decay rate, k_f , of $(\text{Im})(\text{C}_2\text{H}_5\text{OH})\text{Fe}^{\text{II}}\text{TPP}$ observed with the low imidazole concentrations is formulated as $k_f = k_d(1) + k_{bi}(\text{Im}-\text{Im})[\text{Im}]$. The plot of k_f vs $[\text{Im}]$ is identical with that of k_f vs $[\text{Im}]$ as shown in Figure 5. The values of $k_d(1)$ and $k_{bi}(\text{Im}-\text{Im})$ obtained from the photolysis of $(\text{CO})(\text{Im})\text{Fe}^{\text{II}}\text{TPP}$ are in fairly good agreement with those of $(\text{Im})_2\text{Fe}^{\text{II}}\text{TPP}$.

The decay rate constant, k_s , is considered to be a relaxation rate from the first to the second equilibrium. The plot of k_s vs $[\text{Im}]$ is shown in Figure 9. From these equilibria, we obtain

$$-([A] + [B])/dt = k_{bi}(\text{Im}-\text{Im})[A] - k_d(2)[C] \quad (\text{vii})$$

$$k_d(1)/k_{bi}(\text{Im}) = [\text{Im}][B]/[A] \quad (\text{viii})$$

$$[A] + [B] + [C] = C_0 \quad (\text{ix})$$

where A, B, C, and C_0 stand for $(\text{Im})(\text{C}_2\text{H}_5\text{OH})\text{Fe}^{\text{II}}\text{TPP}$, $(\text{C}_2\text{H}_5\text{OH})_2\text{Fe}^{\text{II}}\text{TPP}$, $(\text{Im})_2\text{Fe}^{\text{II}}\text{TPP}$, and total concentration of iron(II) tetraphenylporphyrin. With the use of eqs viii and ix, eq vii is transformed to

$$-d[A]/dt = \{k_{bi}(\text{Im})k_{bi}(\text{Im}-\text{Im})[\text{Im}]^2/(k_d(1) + k_{bi}(\text{Im}) \times [\text{Im}] + k_d(2))\}[A] - k_d(1)k_d(2)C_0/(k_d(1) + k_{bi}(\text{Im})[\text{Im}]) \quad (\text{x})$$

Equation x predicts that the rate constant k_s for the relaxation from the equilibrium 5 to 8 is shown by

$$k_s = k_{bi}(\text{Im})k_{bi}(\text{Im}-\text{Im})[\text{Im}]^2/(k_d(1) + k_{bi}(\text{Im})[\text{Im}]) + k_d(2) \quad (\text{xi})$$

From the computer simulation of the plot of k_s vs $[\text{Im}]$, we obtained $k_d(2) = 3.5 \times 10^3 \text{ s}^{-1}$, $k_{bi}(\text{Im}-\text{Im}) = 7.4 \times 10^6 \text{ M}^{-1} \text{ s}^{-1}$, and $k_{bi}(\text{Im})/k_d(1) = 9.6 \times 10 \text{ M}^{-1}$. The values of $k_{bi}(\text{Im}-\text{Im})$ and $k_d(1)/k_{bi}(\text{Im})$ agree well with those obtained with the laser photolysis of $(\text{CO})(\text{Im})\text{Fe}^{\text{II}}\text{TPP}$ ($6.25 \times 10^6 \text{ M}^{-1} \text{ s}^{-1}$ for $k_{bi}(\text{Im}-\text{Im})$ and $9.2 \times 10 \text{ M}^{-1}$ for $k_{bi}(\text{Im})/k_d(1)$). In Table I, the rate constants obtained by laser photolysis of $(\text{CO})(\text{C}_2\text{H}_5\text{OH})\text{Fe}^{\text{II}}\text{TPP}$, $(\text{CO})(\text{Im})\text{Fe}^{\text{II}}\text{TPP}$, and $(\text{Im})_2\text{Fe}^{\text{II}}\text{TPP}$ are listed. With the use of $k_d(1)$, $k_d(2)$, $k_{bi}(\text{Im})$, and $k_{bi}(\text{Im}-\text{Im})$ in Table I, it was observed that $k_d(1) + k_{bi}(\text{Im})[\text{Im}] \gg k_d(2) + k_{bi}(\text{Im}-\text{Im})[\text{Im}]$ over the whole imidazole concentration range.

The quantum yield for the photodissociation of an axial imidazole from $(\text{Im})_2\text{Fe}^{\text{II}}\text{TPP}$ in ethanol was observed to be as 0.18 at both excitation wavelength 532 and 355 nm.

Temperature-Dependence of Quantum Yields for Photodissociation of Axial Ligands. The quantum yields for photodissociation of CO from $(\text{CO})(\text{C}_2\text{H}_5\text{OH})\text{Fe}^{\text{II}}\text{TPP}$ in ethanol were measured over the temperature range 300–77 K. The yields were independent of temperature for the range 300–140 K. However, the yield dramatically decreased upon going from 140 to 100 K. These

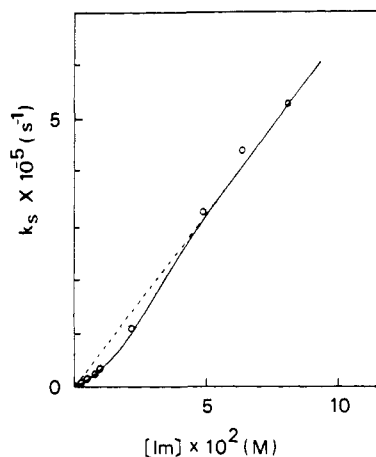
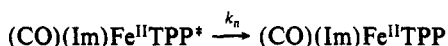
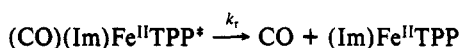


Figure 9. Decay rate constant, k_s , observed with laser photolysis of $(\text{Im})_2\text{Fe}^{\text{II}}\text{TPP}$ in ethanol represented as a function of the imidazole concentration. The solid line is the calculated values of k_d .

results indicated that (1) the activation energy for dissociation of CO at a reactive excited state is almost null in the range 300–140 K and (2) a dramatic decrease in the quantum yields observed below 140 K is probably due to the high viscosity of the solvent ethanol at low temperatures that prevents the dissociation of CO at the reactive state. No excited state of $(\text{CO})(\text{C}_2\text{H}_5\text{O}-\text{H})\text{Fe}^{\text{II}}\text{TPP}$ could be detected below 90 K.

Figure 10 shows the quantum yields for photodissociation of CO from $(\text{CO})(\text{Im})\text{Fe}^{\text{II}}\text{TPP}$ in ethanol in the temperature range 300–180 K. The yields decrease with decreasing temperature. Since the yield shows no excitation wavelength dependence, the reactive excited state responsible for decarbonylation was assumed to be the lowest excited state of $(\text{CO})(\text{Im})\text{Fe}^{\text{II}}\text{TPP}$. From this assumption, the temperature dependence of the quantum yield was considered to originate from the activation process for decarbonylation at the lowest excited state, $(\text{CO})(\text{Im})\text{Fe}^{\text{II}}\text{TPP}^*$.^{18,19} The mechanism for the photodecarbonylation is shown by



The quantum yield, Φ , for the photodecarbonylation is formulated as

$$\Phi = \Phi_L k_r / (k_r + k_n) \quad (\text{xii})$$

where Φ_L is the yield of the lowest excited state. With the use of an Arrhenius expression, k_r is given by

$$k_r = k_r^0 \exp(-\Delta E / RT) \quad (\text{xiii})$$

Here ΔE is the activation energy for decarbonylation at the lowest excited state. Judging from the plot of Φ vs T shown in Figure 9 we consider that Φ at an infinite temperature is almost unity. Thus, Φ_L is safely assumed as $\Phi_L = 1.0$. With the use of eq xiii and $\Phi_L = 1.0$, eq xii is transformed to

$$\ln(1/\Phi - 1) = \ln k_n/k_r^0 + \Delta E/RT \quad (\text{xiv})$$

The plot of $\ln(1/\Phi - 1)$ vs $1/T$ gave a straight line. From the slope and the intercept of the line, we obtained $k_n/k_r^0 = 3.04 \times 10^{-5}$ and $\Delta E/RT = 2.45 \times 10^3$. The quantum yields, therefore, are expressed as

$$\Phi = (1 + 3.04 \times 10^{-5} \exp(2.45 \times 10^3 / T))^{-1} \quad (\text{xv})$$

The solid line in Figure 10 is the quantum yields calculated by eq xv.

Figure 11 shows the quantum yields for photodissociation of Im from $(\text{Im})_2\text{Fe}^{\text{II}}\text{TPP}$, represented as a function of temperature. Because of the fact that the yield for photoejection of Im exhibits no excitation wavelength dependence, we, as in the case of pho-

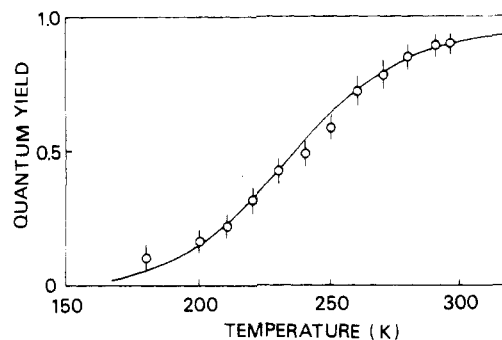


Figure 10. Quantum yields for photodissociation of CO from $(\text{CO})(\text{Im})\text{Fe}^{\text{II}}\text{TPP}$ in ethanol represented as a function of temperature.

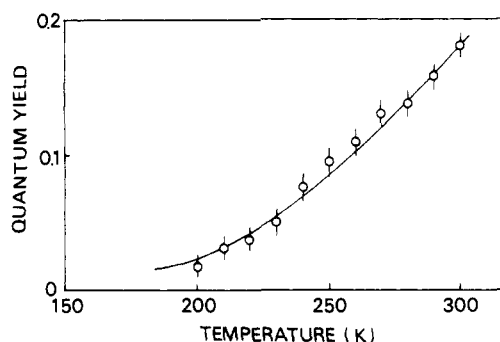


Figure 11. Quantum yields for photodissociation of imidazole from $(\text{Im})_2\text{Fe}^{\text{II}}\text{TPP}$ in ethanol, represented as a function of temperature.

todecarbonylation, assume that (1) the dissociation of Im occurs from the lowest excited state, (2) the yield of the lowest excited state is unity, and (3) there is an activation barrier for ejection of Im from the lowest excited state. From these assumptions, the yield, Φ is well expressed as

$$\Phi = (1 + 5.96 \times 10^{-2} \exp(1.3 \times 10^3 / T))^{-1} \quad (\text{xvi})$$

The solid line in Figure 10 is the quantum yield calculated by eq xvi.

Discussion

Photodecarbonylation. A number of studies on spin multiplicity of iron porphyrins in the ground state have been performed by the measurements of magnetic susceptibilities, ESR, NMR, and Mossbauer spectra.³² It has been demonstrated that (1) carbonyliron(II) porphyrins and $(\text{Im})_2\text{Fe}^{\text{II}}\text{TPP}$ have a spin state of $S = 0$, (2) the spin state of $(2\text{-MeIm})(\text{C}_2\text{H}_5\text{OH})\text{Fe}^{\text{II}}\text{TPP}$ ($2\text{-MeIm} = 2\text{-methylimidazole}$) as well as $(\text{THF})_2\text{Fe}^{\text{II}}\text{TPP}$ ($\text{THF} = \text{tetrahydrofuran}$) is assigned as $S = 2$, and (3) $\text{Fe}^{\text{II}}\text{TPP}$ free from axial ligands, in which the iron atom is strictly centered in the plane of four porphyrinato nitrogens, has a spin state of $S = 1$.³²

We have studied the photolysis of $(\text{CO})(\text{C}_2\text{H}_5\text{OH})\text{Fe}^{\text{II}}\text{TPP}$, $(\text{CO})(\text{Im})\text{Fe}^{\text{II}}\text{TPP}$, and $(\text{Im})_2\text{Fe}^{\text{II}}\text{TPP}$ which have the spin state $S = 0$. The photoproducts yielded immediately after pulsing are considered to be five-coordinate species, $(\text{C}_2\text{H}_5\text{OH})\text{Fe}^{\text{II}}\text{TPP}$ and $(\text{Im})\text{Fe}^{\text{II}}\text{TPP}$, which instantaneously changed to the six-coordinate species, $(\text{C}_2\text{H}_5\text{OH})_2\text{Fe}^{\text{II}}\text{TPP}$ and $(\text{Im})(\text{C}_2\text{H}_5\text{OH})\text{Fe}^{\text{II}}\text{TPP}$. On the basis of the criterion of the axial ligand effects on the spin state of iron(II) porphyrins,³² these five-coordinate species are safely assumed to have a spin state $S = 2$.

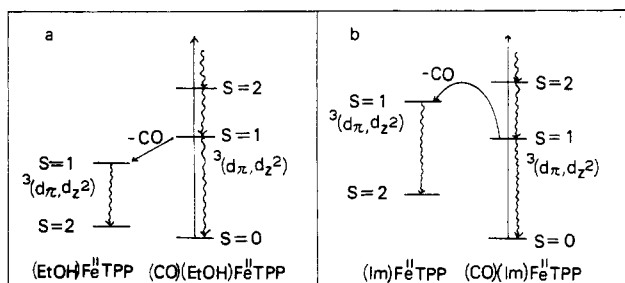
Photodissociation of CO from $(\text{CO})(\text{C}_2\text{H}_5\text{OH})\text{Fe}^{\text{II}}\text{TPP}$ and $(\text{CO})(\text{Im})\text{Fe}^{\text{II}}\text{TPP}$ is considered to occur from the lowest excited state, $^3(d\pi, d_{z^2})^*$.^{18,19} For ejection of CO, the spin-allowed process is expected to be the fastest one. Since the photoinduced decarbonylation products from both $(\text{CO})(\text{C}_2\text{H}_5\text{OH})\text{Fe}^{\text{II}}\text{TPP}$ and $(\text{CO})(\text{Im})\text{Fe}^{\text{II}}\text{TPP}$ are $\text{CO}(^1\Sigma)$ and the five-coordinate species with the spin state $S = 2$, direct ejection of CO from the $^3(d\pi, d_{z^2})^*$ states is predicted to be a spin forbidden process. Here we propose that, as a spin allowed process, decarbonylation from the $^3(d\pi, d_{z^2})^*$ state initially gives $\text{CO}(^1\Sigma)$ and a lowest excited state, $^3(d\pi, d_{z^2})^*$, of $(\text{C}_2\text{H}_5\text{OH})\text{Fe}^{\text{II}}\text{TPP}$ or $(\text{Im})\text{Fe}^{\text{II}}\text{TPP}$ which finally relaxes to

TABLE I: Rate and Equilibrium Constants for Association and Dissociation of Axial Ligands in Ethanol

$(C_2H_5OH)_2Fe^{II}TPP + CO \rightarrow (CO)(C_2H_5OH)Fe^{II}TPP + C_2H_5OH$	$k_{bi}(CO) = 1.0 \times 10^7 M^{-1} s^{-1} a,b$
$(C_2H_5OH)_2Fe^{II}TPP + Im \rightarrow (Im)(C_2H_5OH)Fe^{II}TPP + C_2H_5OH$	$k_{bi}(Im) = 1.1 \times 10^8 M^{-1} s^{-1} b,c$
$(Im)(C_2H_5OH)Fe^{II}TPP + Im \rightarrow (Im)_2Fe^{II}TPP + C_2H_5OH$	$k_{bi}(Im-Im) = 6.3 \times 10^6 M^{-1} s^{-1} b$
$(CO)(C_2H_5OH)Fe^{II}TPP + Im \rightarrow (Im)(CO)Fe^{II}TPP + C_2H_5OH$	$k_{bi}(Im-Im) = 7.4 \times 10^6 M^{-1} s^{-1} c$
$(Im)(C_2H_5OH)Fe^{II}TPP + C_2H_5OH \rightarrow (C_2H_5OH)_2Fe^{II}TPP + Im$	$k_{bi}(CO-Im) = 1.52 \times 10^5 M^{-1} s^{-1} b$
$(Im)_2Fe^{II}TPP + C_2H_5OH \rightarrow (Im)(C_2H_5OH)Fe^{II}TPP + Im$	$k_d(1) = 1.2 \times 10^6 s^{-1} b,c$
$(C_2H_5OH)_2Fe^{II}TPP + Im \rightleftharpoons (Im)(C_2H_5OH)Fe^{II}TPP + C_2H_5OH$	$k_d(2) = 3.5 \times 10^3 M^{-1} s^{-1}$
$(Im)(C_2H_5OH)Fe^{II}TPP + Im \rightleftharpoons (Im)_2Fe^{II}TPP + C_2H_5OH$	$K_1 = k_{bi}(1)/k_d(1) = 9.2 \times 10 M^{-1} b$
$(C_2H_5OH)_2Fe^{II}TPP + 2 Im \rightleftharpoons (Im)_2Fe^{II}TPP + 2 C_2H_5OH$	$K_1 = k_{bi}(1)/k_d(1) = 9.6 \times 10 M^{-1} c$
	$K_2 = k_{bi}(Im-Im)/k_d(2) = 2.1 \times 10^3 M^{-1} c$
	$K = 2.0 \times 10^5 M^{-2} d$
	$K = K_1 \times K_2 = 2.0 \times 10^5 M^{-2} c$

^a Values obtained from laser photolysis of $(CO)(C_2H_5OH)Fe^{II}TPP$. ^b Values obtained from laser photolysis of $(CO)(Im)Fe^{II}TPP$. ^c Values obtained from laser photolysis of $(Im)_2Fe^{II}TPP$. ^d Values obtained from the absorption spectral changes of $(C_2H_5OH)_2Fe^{II}TPP$ as a function of $[Im]$.

SCHEME II



the ground state $S = 2$. The quantum yield measurements at various temperatures have revealed that $(CO)(C_2H_5OH)Fe^{II}TPP$ has no activation barrier for photodecarbonylation in the range 300–180 K, while $(CO)(Im)Fe^{II}TPP$ has an activation energy of 4.5 kcal mol⁻¹. This result is interpreted by assuming that (1) the energy of the $^3(d\pi, d_z^2)^*$ state of $(C_2H_5OH)Fe^{II}TPP$ is lower than that of $(CO)(C_2H_5OH)Fe^{II}TPP$ and (2) the energy of the $^3(d\pi, d_z^2)^*$ state of $(Im)Fe^{II}TPP$ is higher than that of $(CO)(Im)Fe^{II}TPP$. The photodissociation mechanism of CO is represented in Scheme II.

Photolysis of $(Im)_2Fe^{II}TPP$ readily liberates an axial imidazole. Since $(Im)_2Fe^{II}TPP$ and the initial photoproduct, $(Im)Fe^{II}TPP$, may have the spin state $S = 0$ and $S = 2$, respectively, direct dissociation of imidazole from the lowest excited state, $^3(d\pi, d_z^2)^*$, of $(Im)_2Fe^{II}TPP$ is a spin forbidden process. It is likely, as in the case of $(CO)(Im)Fe^{II}TPP$, that $(Im)_2Fe^{II}TPP$ in the $^3(d\pi, d_z^2)^*$ state initially yields Im and $(Im)Fe^{II}TPP$ in the $^3(d\pi, d_z^2)^*$ state with an activation energy of 2.6 kcal mol⁻¹. The energy of the $^3(d\pi, d_z^2)^*$ state of $(Im)Fe^{II}TPP$ is presumably higher than that of $(Im)_2Fe^{II}TPP$.

Spontaneous Dissociation of Axial Bases. Five-coordinate iron(II) porphyrin, $(B)Fe^{II}P$ ($B =$ axial base and $P =$ porphyrin), which is produced by laser photolysis of $(CO)(B)Fe^{II}P$ or $(B)_2Fe^{II}P$ in toluene, is known to undergo the spontaneous dissociation of an axial base B to give $Fe^{II}P$.^{15,25}

We also observed spontaneous dissociation of the axial base from $(Im)(C_2H_5OH)Fe^{II}TPP$ in ethanol produced by photolysis of $(CO)(Im)Fe^{II}TPP$ and $(Im)_2Fe^{II}TPP$ at low concentrations of imidazole. Because the photoreaction system of $(Im)_2Fe^{II}TPP$ is more simple than that of $(CO)(Im)Fe^{II}TPP$, we discuss the spontaneous dissociation on the basis of the laser photolysis studies of $(Im)_2Fe^{II}TPP$. As previously shown in Scheme I, the laser photolysis of $(Im)_2Fe^{II}TPP$ gives $(Im)(C_2H_5OH)Fe^{II}TPP$ as the initial observable product. The product, $(Im)(C_2H_5OH)Fe^{II}TPP$, establishes an equilibrium with both $(C_2H_5OH)_2Fe^{II}TPP$ and $(Im)_2Fe^{II}TPP$. We found that a second equilibrium between $(Im)(C_2H_5OH)Fe^{II}TPP$ and $(Im)_2Fe^{II}TPP$ is established after achievement of the first equilibrium between $(Im)(C_2H_5OH)Fe^{II}TPP$ and $(C_2H_5OH)_2Fe^{II}TPP$. This finding implies that the rate constant for establishment of the first equilibrium is much larger than that of the second equilibrium: $k_d(1) + k_{bi}(Im)[Im] \gg k_d(2) + k_{bi}(Im-Im)[Im]$. Thus, when $[Im]$ is low, spontaneous dissociation of imidazole from $(Im)(C_2H_5OH)Fe^{II}TPP$ can be observed. The relationship $k_d(1) + k_{bi}(Im)[Im] \gg k_d(2) +$

$k_{bi}(Im-Im)[Im]$ can be interpreted in terms of the spin state of $(Im)(C_2H_5OH)Fe^{II}TPP$ ($S = 2$), $(C_2H_5OH)_2Fe^{II}TPP$ ($S = 2$), and $(Im)_2Fe^{II}TPP$ ($S = 0$). The first equilibrium between $(Im)(C_2H_5OH)Fe^{II}TPP$ ($S = 2$) and $(C_2H_5OH)_2Fe^{II}TPP$ ($S = 2$) is considered to be the spin allowed process for forward and backward reactions, while the second equilibrium between $(Im)(C_2H_5OH)Fe^{II}TPP$ ($S = 2$) and $(Im)_2Fe^{II}TPP$ ($S = 0$) is the spin forbidden process. The assumption that the rate constant of the spin allowed reaction is large in comparison with that of the spin forbidden reaction leads to $k_d(1) \gg k_d(2)$ for the dissociation process of imidazole and $k_{bi}(Im) \gg k_{bi}(Im-Im)$ for the association process of imidazole, i.e., $k_d(1) + k_{bi}(Im)[Im] \gg k_d(2) + k_{bi}(Im-Im)[Im]$.

Acknowledgment. We thank Dr. J. P. Lillis for his critical reading of the manuscript.

References and Notes

- (1) Kim, D.; Holten, D.; Gouterman, M. *J. Am. Chem. Soc.* **1984**, *106*, 2793–2798.
- (2) Hoshino, M.; Seki, H. *Chem. Phys. Lett.* **1984**, *110*, 413–416.
- (3) Straub, K.; Rentzepis, P. M.; Huppert, D. *J. Photochem.* **1981**, *17*, 419–425.
- (4) Tait, C. D.; Gouterman, M.; Holten, D. *Chem. Phys. Lett.* **1983**, *100*, 268–272.
- (5) Guest, C. R.; Straub, K. D.; Hatchinson, J. A.; Rentzepis, P. M. *J. Am. Chem. Soc.* **1988**, *110*, 5276–5280.
- (6) Yamaji, M.; Hama, Y.; Hoshino, M. *Chem. Phys. Lett.* **1990**, *165*, 309–314.
- (7) Hoshino, M.; Kogure, M.; Amano, K.; Hinohara, T. *J. Phys. Chem.* **1989**, *93*, 6655–6659.
- (8) Tetreau, C.; Lavalette, D.; Momenteau, M. *J. Am. Chem. Soc.* **1983**, *105*, 1505–1509.
- (9) Tait, C. D.; Holten, D.; Gouterman, M. *J. Am. Chem. Soc.* **1984**, *106*, 6653–6659.
- (10) Kim, D.; Kirmaier, C.; Holten, D. *Chem. Phys.* **1983**, *75*, 305–322.
- (11) Hoshino, M.; Seki, H.; Yasufuku, K.; Shizuka, H. *J. Phys. Chem.* **1986**, *90*, 5149–5153.
- (12) Collman, J. P.; Gagne, R. R.; Reed, C. A.; Halbert, T. R.; Lang, G.; Robinson, W. T. *J. Am. Chem. Soc.* **1975**, *97*, 1427–1439.
- (13) Hoshino, M.; Kogure, M. *J. Phys. Chem.* **1989**, *93*, 5478–5484.
- (14) Vogler, A.; Kunkely, H. *Ber. Bunsen-Ges. Phys. Chem.* **1976**, *80*, 425–429.
- (15) White, D. K.; Cannon, J. B.; Traylor, T. G. *J. Am. Chem. Soc.* **1979**, *101*, 443–2454.
- (16) Dlott, D. D.; Frauenfelder, H.; Langer, P.; Roder, H.; Dilorio, E. E. *Proc. Natl. Acad. Sci. U.S.A.* **1983**, *80*, 6239–6243.
- (17) Hoffman, B. M.; Gibson, Q. H. *Proc. Natl. Acad. Sci. U.S.A.* **1978**, *75*, 21–25.
- (18) Chernoff, D. A.; Hochstrasser, R. M.; Steele, L. W. *Proc. Natl. Acad. Sci. U.S.A.* **1980**, *77*, 5606–5610.
- (19) Greene, B. I.; Hochstrasser, R. M.; Weisman, R. B.; Eaton, W. A. *Proc. Natl. Acad. Sci. U.S.A.* **1978**, *75*, 5255–5259.
- (20) Parkhurst, L. J.; Gross, D. *J. Biochemistry* **1984**, *23*, 2180–2186.
- (21) Duddle, D. A.; Morris, R. J.; Richard, J. T. *J. Chem. Soc., Chem. Commun.* **1979**, 75–76.
- (22) Hasinoff, B. B. *J. Phys. Chem.* **1981**, *85*, 526–531.
- (23) Cornelius, P. A.; Hochstrasser, R. M.; Sycle, A. W. *J. Mol. Biol.* **1983**, *163*, 119–128.
- (24) Alpert, B.; El Mohshi, S.; Lindquist, L.; Tfibel, F. *Chem. Phys. Lett.* **1979**, *64*, 11–16.
- (25) Lavalette, D.; Tetreau, C.; Momenteau, M. *J. Am. Chem. Soc.* **1979**, *101*, 5395–5401.
- (26) Dorough, D. G.; Miller, J. R.; Huennekens, F. M. *J. Am. Chem. Soc.* **1951**, *73*, 4315–4320.
- (27) Hoshino, M.; Ueda, K.; Takahashi, M.; Yamaji, M.; Hama, Y. *J.*

Chem. Soc., Faraday Trans. 1992, 88, 405-408.

(28) Hoshino, M.; Imamura, M.; Watanabe, S.; Hama, Y. *J. Phys. Chem.* 1984, 88, 45-49.

(29) Hurley, J. K.; Sinai, N.; Linschitz, H. *Photochem. Photobiol.* 1983, 38, 9-14.

(30) *Kagaku Benran*; Hata, K., Ed.; Maruzen, Tokyo, 1984; Vol. 2,

Chapter 8.

(31) Brault, D.; Rougee, M. *Biochemistry* 1974, 13, 4591-4597.

(32) *The Porphyrins*; Dolphin, D., Ed.; Academic Press: New York, 1978; Vol. 4.

(33) Sams, J. R.; Tsin, T. S. In *The Porphyrins*; Dolphin, D., Ed.; Academic Press: New York, 1978; Vol. 4, Chapter 9.

Translational Energy-Resolved Collisionally Activated Methyl Cation Transfer from Protonated Methane to Argon, Krypton, and Xenon and from Protonated Fluoromethane to Argon and Molecular Oxygen

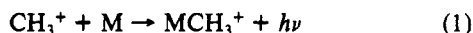
Albert J. R. Heck, Leo J. de Koning, and Nico M. M. Nibbering*

Institute of Mass Spectrometry, University of Amsterdam, Nieuwe Achtergracht 129, 1018 WS Amsterdam, The Netherlands (Received: April 9, 1992; In Final Form: July 10, 1992)

Translational energy-resolved collisionally activated gas-phase reactions of protonated methane with argon, krypton, and xenon and of protonated fluoromethane with argon and molecular oxygen are studied using the method of Fourier transform ion cyclotron resonance mass spectrometry. It appears that translationally activated protonated methane can act as a methyl cation donor if the competing proton transfer is energetically less favored. Translational energy-resolved collisionally activated reactions between protonated methane and argon, krypton, and xenon reveal that the methyl cation transfers resulting in the formation of methylargonium, methylkryptonium, and methylxenonium ions all proceed via transition states which are about 0.6 eV higher in energy than the reactants. The results suggest that in these transition states the weakening of the two-electron three-center C-H-H bond in protonated methane is more advanced than the bond formation between the methyl group and the noble gas atom. Similarly, translationally activated protonated fluoromethane can transfer a methyl cation to argon and molecular oxygen via transition states which are about 0.3 and 0.4 eV higher in energy than the reactants, respectively. It is shown that the product ion from the methyl cation transfer from protonated fluoromethane to molecular oxygen has the methylperoxy cation structure.

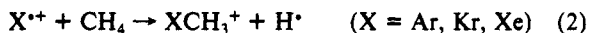
Introduction

Radiative association reactions of the methyl cation with various molecules M (eq 1) are considered to be the first stages in the



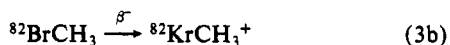
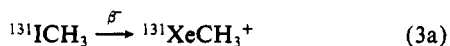
synthesis of some important interstellar molecules, where M may be H₂, Ne, O₂, CO, CO₂, N₂, HCN, NH₃, etc.¹⁻⁶ This significance in interstellar processes has led to several laboratory studies of methyl cation transfer equilibria reactions,³⁻⁸ from which a methyl cation affinity (MCA) scale has been established.^{8,9}

Methyl Cationized Noble Gases. The first observations of methyl-cationized noble gases were made by Field et al.¹⁰⁻¹² in studies of the ionic reactions in a mass spectrometer with noble gas/methane mixtures. The ions were formed via the ion/molecule reactions (eq 2). The results were reproduced by Jonathan et al.,¹³



who characterized the observed methyl-cationized argon, krypton, and xenon by collision-induced dissociation. To our knowledge no observation of the methyl-cationized neon or helium has been reported.

Alternatively, methyl-cationized noble gases have been generated via β^- decay of the corresponding isoelectronic radioactive halomethanes (eq 3)¹⁴ Holtz et al. demonstrated the formation



of methyl-cationized xenon in the reaction between xenon and protonated fluoromethane (eq 4a),¹⁵ whereas Hovey et al.¹⁶

generated methyl-cationized krypton by similar processes (eqs 4b and 4c).



The methyl cation affinities (MCA) have been determined from gas-phase methyl cation transfer equilibrium measurements and found to be 2.2 and 1.9 eV for xenon and krypton, respectively.^{8,16} These MCA's indicate that the "inert" noble gas atoms can establish a remarkably strong bond with the methyl cation which can be considered to have covalent character.

The generally found simple linear relationship between ionization energies, gas-phase proton affinities, and/or methyl cation affinities^{8,16} led to the suggestion that also methylated argon cations would be energetically accessible via a reaction between protonated fluoromethane and argon as follows from the data presented in Figure 1. This figure shows proton affinities (PA) and methyl cation affinities (MCA) of the noble gases, and for comparison, of the hydrogen halides, as a function of their ionization energies.

Since an excellent linear relationship is found between the proton affinities of the noble gases and their ionization energies (Figure 1) it seems reasonable to anticipate a linear relationship between the methyl cation affinities and the ionization energies of the noble gases as well. Based on the methyl cation affinities of xenon and krypton as determined from methyl cation transfer equilibrium measurements (see above), a linear relationship predicts the methyl cation affinity of argon to be about 1.6 eV, which is larger than the experimentally determined methyl cation affinity of hydrogen fluoride of 1.5 eV^{8,9} (Figure 1). Yet, in the reaction between protonated fluoromethane and argon only a trace of the possible methylated argon product ion has been observed under ambient temperature conditions.^{8,16}

* Author to whom correspondence should be addressed.